PIV MEASUREMENTS OF THE VORTICAL STRUCTURES IN ROTATING CHANNELS

Alberto Di Sante [(*)], René A. Van den Braembussche, Tony Arts
von Karman Institute for Fluid Dynamics
Waterloose Steenweg, 72
Sint-Genesius-Rode, BELGIUM
alberto.di-sante@power.alstom.com, vdb@vki.ac.be , arts@vki.ac.be

ABSTRACT

A new facility for 2D, Time-Resolved PIV measurements of low Reynolds number flows in rotating channels with heat transfer is presented. It allows measuring the impact of Coriolis forces on the flow in centrifugal impellers of micro gas turbines and internal cooling channels of conventional HP turbines blades.

Measurements are taken by means of a continuous laser diode, coupled by fiber optics to an optics module, and a high speed CMOS camera mounted together with the channel on a 2.5m diameter rotating disk. This allows a direct measurement of the relative velocity and the time evolution of the 2D vortical structures. The results provide input for improved turbulence modeling and LES computations.

The advantage of the rotating instrumentation is a reduction of the error of the instantaneous PIV measurements and the possibility to trace the vortical structures. The possibility to heat the channel walls, while preserving optical access, is a future development of the facility.

INTRODUCTION

CFD is intensively used for the design of centrifugal compressors for micro gas turbines and internal cooling channels in large HP turbines. However, the turbulence models implemented in those solvers are mostly based on experimental data obtained in stationary geometries at high Reynolds number and do not account for curvature and rotational effects. Johnston, one of the first experimenters to provide measurements in rotation [1,2], defined in 1998 the state of the art in turbulence modeling for the flow in rotating channels as “rather primitive”. A large progress has been made since then [3], but detailed experimental data for validation are still very scarce.

Several studies report about the measurement of the relative velocity in rotating channels [4,5,6]. However the point wise hot-wire and pressure probe measurements cannot resolve the vortical structures. This was remediated by Bons and Kerrebrock [7,8] who made phase-locked Particle Image Velocimetry (PIV) measurements of the absolute velocity in the peripheral plane of a rotating channel by triggering a stationary CCD camera and Nd-YAG laser at each passage of the channel. However, a correct computation of the absolute velocity vectors requires a rotation of the second image, which according to Bons [7] introduces a bias error of the order of 4%. As will be discussed later in this paper, the transformation of the measured absolute velocities into relative ones constitutes an even larger source of error. Furthermore, at large peripheral velocities, the channel wall displacement in the field-of-view of the stationary camera leads to a decreasing area where velocity vectors can be retrieved. The difficulty to measure close to the moving lateral walls prevent a proper resolution of the boundary layers required for an accurate estimation of the turbulence intensity distributions.

The main shortcomings of previous experimental results are an insufficient temporal and inaccurate spatial resolution of the flow required for a detailed description of the fluid mechanics of low Reynolds number flows in rotating channels. The new facility described in this paper intends to fill that gap. It is a follow up of the extensive experimental and numerical research in stationary models of the aerodynamic and thermal aspects of internal cooling channel flows [9,10] as well as PIV measurements in centrifugal impellers [11]. The results allow verifying the accuracy of the numerical predictions and provide information for the improvement and validation of turbulence models.

Next section presents the new rotating facility and its instrumentation. It is further shown that a direct measurement of the relative velocity in the rotating frame results in a drastic improvement of the accuracy. The impact of rotation on turbulence and vortical structures is illustrated by the detailed measurements obtained in a low aspect-ratio diverging channel. Conclusions and future development of the facility, involving heating of the channel walls, are a last part of the paper.

[(*)] Presently at ALSTOM Power, Switzerland

THE RC-1 FACILITY AND INSTRUMENTATION

Description of the facility

A 0.7 m long rectangular channel is mounted on a 2.5 m disk rotating around a horizontal axis (Fig. 1). Dependent on its divergence angle, it models the interblade channel of a micro gas turbine centrifugal compressor impeller or the internal cooling passage of a large HP turbine. The channel has 0.01 m thick Plexiglas walls and an inlet section of 0.075×0.083 m^2. The wall on which the laser light impinges is made of polished steel. The precise light reflection avoids stray light scatter and increases the intensity of the light in the measurement area. The backside wall is covered with a matt black adhesive sheet to avoid background light reflections. A variable speed DC motor rotates the disk up to maximum 160 rpm.

A fine mesh honeycomb (3mm cell diameter) reduces the flow disturbances downstream of the 90° turn at the exit of the rotating duct. The length of the honeycomb is 40 mm which is more than 10 times the cell size [12]. A fine grid at 10 mm distance downstream of the honeycomb merges the individual honeycomb wakes. The space between the honeycomb and the grid is less than 5 times the cell size as recommended in [12,13]. A second mesh at the outlet of the diffuser (cell size: 8 mm) reduces the lateral cross flow due to channel vorticity (slip) and the absence of periodicity in geometry and flow.

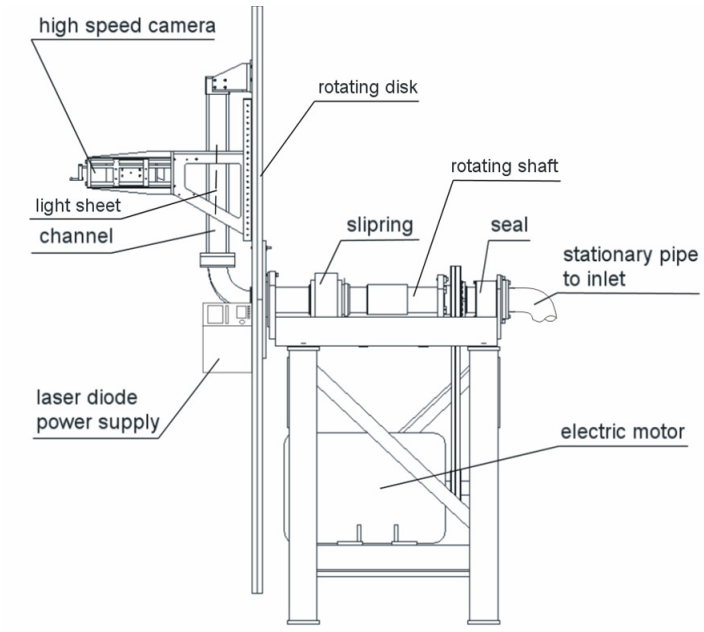

Fig. 1 Sketch of the RC1 rotating facility

The desired channel inlet velocity is calculated from the volume flow measured with a Venturi and is controlled by a variable speed blower and throttling valve in the stationary pipe. The throttling valve is needed when the rotating channel creates a larger pressure rise than the one corresponding to the required volume flow. A rotary seal connects this stationary pipe with the rotating hollow shaft. The 10-channel slip ring from 'IEC Corporation' model D-1370 is used only to transmit the 220 V electrical power and triggering signals to the rotating disk. Static balancing of the disk proved to be sufficient up to 160 RPM. It is performed by moving some of the 6 steel blocks of 3 kg each along two radial rails to compensate for the different positions of the high-speed camera.

The PIV seeding is generated by an in-house built device producing vaporized oil particles with a diameter in the range of 1 to 6 μm. Uniform mixing in the test section is achieved by injecting the smoke shortly upstream of the rotating shaft. The seeding coming out of the rotating channel is collected by a stationary circumferential passage and aspirated by a centrifugal blower. The same structure also serves safety purposes.

Table 1 Typical parameters for a μ GT impeller, cooling channel and model of the RC-1 facility

	W_{in} [m/s]	$d_{h,in}$	ρ [kg/m^3]	rpm	Re	Ro
μ impeller	280	0.0007	1.3	500,000	13,166	0.26
cooling channel	20	0.0025	11.0	13,000	14,500	0.34
model	2.5	0.079	1.3	40	13,166	0.26

Table 1 illustrates how this facility allows simulation of the flow at Reynolds ($\mathrm{Re} = \frac{W_{in} d_{h,in}}{\upsilon}$) and rotation numbers ($Ro = \frac{2\omega d_{h,in}}{W_{in}}$) that are representative for micro gas turbines and cooling channels.

Instrumentation

Time- Resolved Particle Image Velocimetry (TR-PIV) is an experimental technique still in a development phase. Water cooled high-energy pulsed lasers have large dimensions and weight and cannot be mounted on rotating disks. An alternate solution is to make the laser light rotate with the test section by a mirror mounted on the rotation axis [14,15]. These systems are very sensitive to vibrations and risk of losing the alignment. This problem could be avoided by using fiber optic cables and a rotating optical encoder mounted on the facility axis. However, the oil used in those encoders to transmit the light from the rotor to the stationary part, vaporizes by the high power laser light. The use of multimode fibers of large diameter, to transmit the high power light pulses and continuous laser light, was proven possible [16,17] but the measurement quality was not discussed in detail

Mounting a CCD camera on the rotating disk poses the problem of the data transmission to the stationary acquisition card. The high data rate (≈140 Mbytes/s) is at the verge of the capabilities of electrical slip rings and optical encoders. Moreover there is in both cases a high risk to introduce noise. The very high data rate also prevents the use of a frequency transmitter. It is concluded from this that the optimum solution to perform direct relative velocity measurements with the PIV technique is by means of a compact, air-cooled laser light source and a camera with an internal memory.

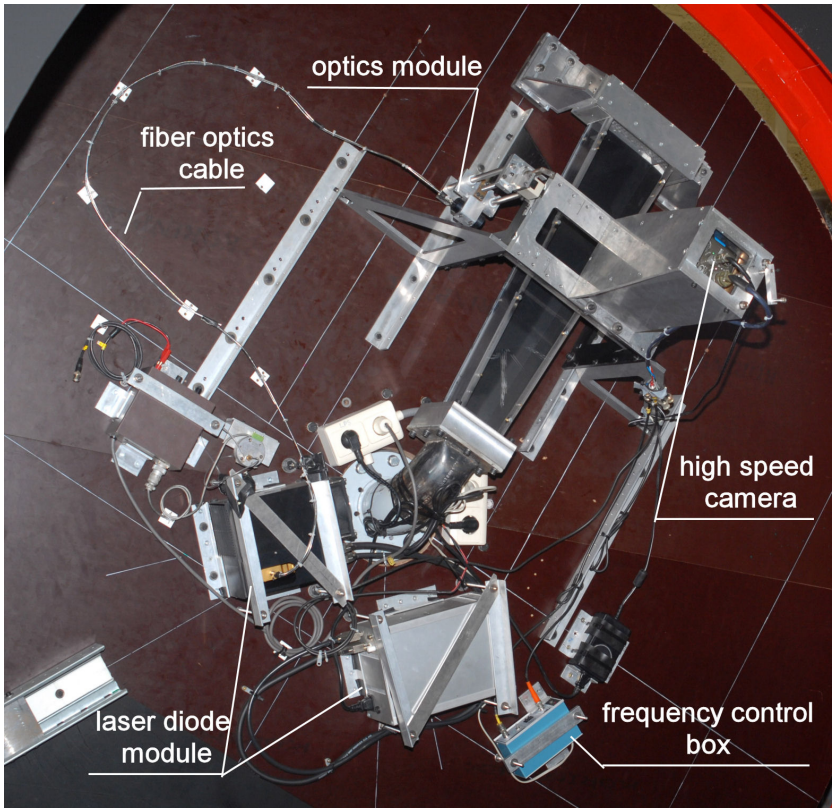

Fig. 2 Frontal view on the RC1 rotating facility and TR-PIV system

A laser diode system is chosen because it meets all the specified requirements: it is compact, light and air-cooled. It operates at low voltages (2-3 Volts) but high Amperes (up to 40 A) and produces a highly divergent, elliptical and astigmatic light beam. The selected laser diode module is from “Unique Mode” (now “Jenoptik”) [18]. It consists of the ‘VAS00300’ power supply and the 25 Watt air-cooled ‘UM25k’ laser diode (Fig. 2) providing light at 806 nm wavelength. The impact of the wavelength on the measurement quality can be assessed by Mie’s theory, requiring that the particle diameter must be larger than the wavelength of the laser light. This is not a problem as the vaporized oil particles have a diameter d_p between 1 and 6 µm. The average energy of the scattered light is proportional to $(d_p/\lambda)^2$. This means that the energy scattered from particles illuminated by a 25 W laser at 806 nm is equivalent to the energy scatter obtained with 10 W laser at 512 nm (at

unchanged particle diameter, lens aperture and magnification factor). However compact, air cooled laser diode modules with a 500 nm wavelength have a maximum power of ≈5 W and are 10 times more expensive than laser diode modules emitting at 800 nm. The laser diode and the power supply are fixed on the disk close to the axis of rotation (Fig. 1 and Fig. 2).

A multimode optical fiber with 200 μm core diameter and a numerical aperture of 0.22 transmits the laser light to a compact optics module built on specific request by Jenoptik. The latter generates a homogeneous light sheet with 16° total aperture angle without noticeable speckle. 75% of the light power is contained within a sheet of 1mm thickness of the 40x 40 mm^2 measurement zone. A larger measurement zone is not possible because of the rapid increase of the minimum waist. The fiber is fixed on the disk to eliminate any change in light sheet properties. The laser plane forming optics and the camera are mounted on a structure that can be displaced radially, tangentially and vertically to measure at all locations along the channel and planes over the channel height.

The Vision Research "Phantom" 7.1 CMOS high-speed camera is a "stand alone" device storing images in its 1GB internal memory (expandable to 8 GB) [19]. The sampling frequency can go up to 7.3 kHz at a resolution of 640× 480 $pixel^2$. The only connection to an external device is by the trigger signal. Collecting and storing the data in the same frame of reference eliminates any transmission noise. The objective is a 50 mm, f/1.8 Nikon Nikkor combined with a 12mm extension ring. The lens has to be used at its maximum aperture since the energy released from the laser diode during a typical exposure time of 150 μs is only 4 mJ.

Experimental procedure

The RC-1 facility is run in isothermal conditions using ambient air. The TR-PIV measurements have been performed at mid channel height in a plane halfway between the inlet and outlet of a 6°diverging channel. Conformal to turbomachinery terminology, the lateral walls will be referred to as pressure (or leading) side (PS) and suction (or trailing) side (SS) (Fig.3).

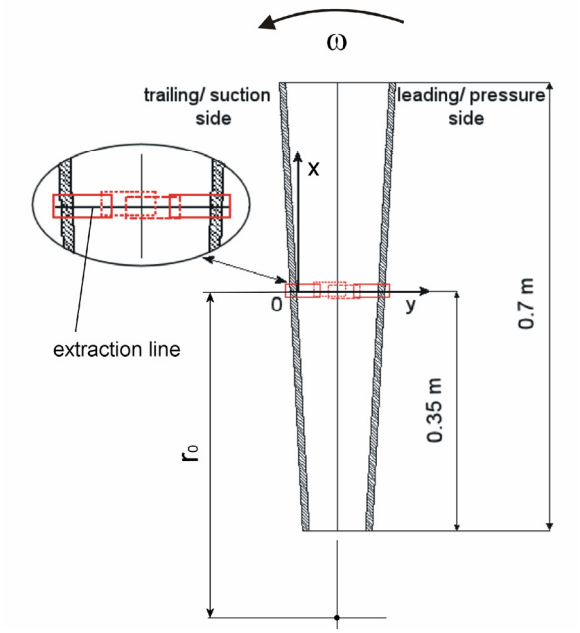

Fig. 3 Measurement zones

The field of view used for the results presented in this paper is 20.86× 45.2 mm^2 corresponding to an image of 240× 520 $pixel^2$. It means that four slightly overlapping zones are required to measure the whole passage between SS and PS. When changing the sense of rotation the SS becomes a PS and vice versa, so that only two positions of the optics and the camera are needed to cover the whole channel width.

A correct reproduction of the mean flow field requires a sufficiently large number of single measurements to filter out the unsteadiness of the flow. The maximum number of samples is limited by the memory of the camera and the size of the images. Decreasing the resolution of the camera could allow an increase of the number of measurements but at the cost of a lower accuracy.

The exposure time '*dt*' can be varied independent of the acquisition frequency. This allows controlling the amount of light collected on each image when using a continuous laser light source. This is needed to obtain a correct seeding particle size in terms of sensor pixels and good intensity peaks in the stored images. In order to maximize the accuracy of the image processing, the separation time 'Δt' of the camera, (Fig. 4) is adjusted to

obtain a particle image displacement of about 8-10 pixels [20]. An electronic device, gating the writing operation of the camera memory, allows setting the sampling frequency f_s independently from the separation time (Fig. 4). This feature allows an increase of the cut-off time required for converged flow statistics. In total 2,777 image couples were recorded for each single measurement.

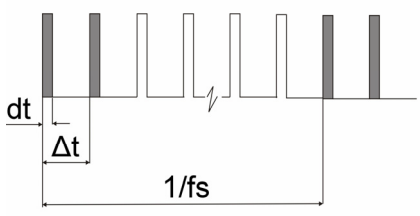

Fig. 4 Time settings for the TR-PIV measurement

Following results are obtained for rotational speeds of 0 and 40 rpm and the flow characteristics specified in Table 1. The measurement parameters are summarized in Table 2. A detailed description of data reduction can be found in [21,22]

Table 2 Measurement parameters

dt [μs]	Δt [μs]	cut-off time [s]	f_s [Hz]	FOV [pixels]
140	463	7.8	360	240 × 520

MEASUREMENT ACCURACY

The main advantage of the present system is its capacity to measure directly the relative velocity. This does not only avoid the 4% bias error, mentioned by Bons [7], but also eliminates the errors related to the calculation of the relative velocity component 'W' by subtracting the peripheral velocity '$U=\omega \cdot r$' from the measured absolute velocity 'V' (Fig. 5).

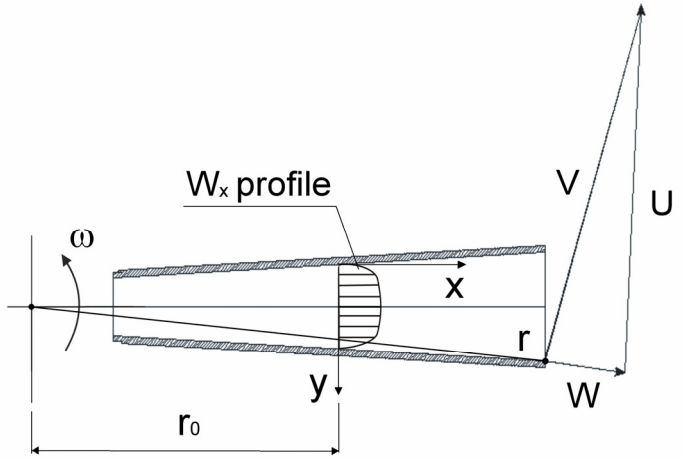

Fig. 5 Velocity triangle for a the flow in a rotating channel and imposed relative velocity profile

Following estimates these losses assuming that all other sources of uncertainty are not influenced by this change in measurement plane and that the same measurement zone requires the same magnification factor 'M'. The measured absolute velocity $V = \frac{\Delta s \cdot M}{\Delta t_{abs}}$ relates to the relative velocity $W = \sqrt{\left(\frac{\Delta s \cdot M}{\Delta t_{abs}}\right)^2 - (\omega \cdot R)^2}$. The error on the relative velocity can be expressed in terms of the error on the pixel displacement between successive recordings *'Δs'* as $\varepsilon_{W|abs} = \frac{1}{W} \cdot \frac{\Delta s \cdot M}{\Delta t_{abs}} \cdot \frac{M \cdot \varepsilon_{\Delta s}}{\Delta t_{abs}}$ or $\varepsilon_{W|abs} = \frac{V}{W} \cdot \frac{M \cdot \varepsilon_{\Delta s}}{\Delta t_{abs}}$. Analysis of the PIV recordings by means of cross-correlation algorithms is in average accurate up to one tenth of a pixel with a

maximum precision of 0.05 pixels [23]. The envelope of maximum uncertainty is thus given as $\varepsilon_{\Delta s} \le \sqrt{0.1^2 + t \cdot 0.05^2}$ where 't' is the Student 't' value corresponding to a confidence level of 95% [24].

In a direct measurement, the relative velocity is defined by $W = \frac{\Delta s \cdot M}{\Delta t_{rel}}$ and the error on the velocity relates to the error on the image displacement by $\varepsilon_{W|rel} = \frac{M \cdot \varepsilon_{\Delta s}}{\Delta t_{rel}}$. To limit the out-of-plane loss of particles it is standard practice to adjust the separation times *'Δt_{rel}'* and *'Δt_{abs}'* such that the maximum encountered velocities, respectively *'W_{max}'* and *'V_{max}'*, do not exceed a 8 to 10 pixel displacement [20]. Hence the error on the 'W' velocity component measured in the absolute frame relates to the one derived from the direct relative velocity measurement as

$$\frac{\varepsilon_{W|abs}}{\varepsilon_{W|rel}} = \frac{V}{W} \cdot \frac{M}{\Delta t_{abs}} \cdot \frac{\Delta t_{rel}}{M} = \frac{V}{W} \cdot \frac{V_{max}}{10\,pix} \cdot \frac{10\,pix}{W_{max}} = \frac{V}{W} \cdot \frac{V_{max}}{W_{max}}$$

This ratio consists of two parts. The first one increases with the ratio between absolute and local relative velocities ('V/W') and is a function of the imposed flow conditions. The value of V being always larger than U, this contribution becomes very large in the boundary layer where W goes to zero. The second part ('V_{max}/W_{max}') relates to the adjustment in separation time when changing reference frame.

The improvement in relative uncertainty is illustrated by means of a typical relative velocity profile 'W_x' with a free stream velocity of 1.163 m/s and a boundary layer thickness 'δ_{BL}' of 15 mm. The radial distance of the measurement plane from the axis of rotation 'r_0' is 0.5 m. The effect of increasing rotational speed on the measurement error is shown in Fig. 6a. The uncertainty distribution for the direct measurement of the relative velocity in the rotating facility is independent of the rotational velocity. The smallest uncertainties (2%) are observed in the free stream. The gradual increase, when approaching the wall, is due to the decrease of the particle displacements in the boundary layer. For the measurements made with a fixed PIV system, the minimum errors vary from 8% to 25% and 95% at respectively 40, 80 and 160 rpm.

A similar tendency (Fig. 6b) is observed when varying the radial position of the measurement for a given rotational speed (40 rpm). The minimum bulk flow uncertainty reaches values of 8%, 17% and 30% when measuring with a fixed PIV system at a radius of 0.5, 0.675 and 0.85m.

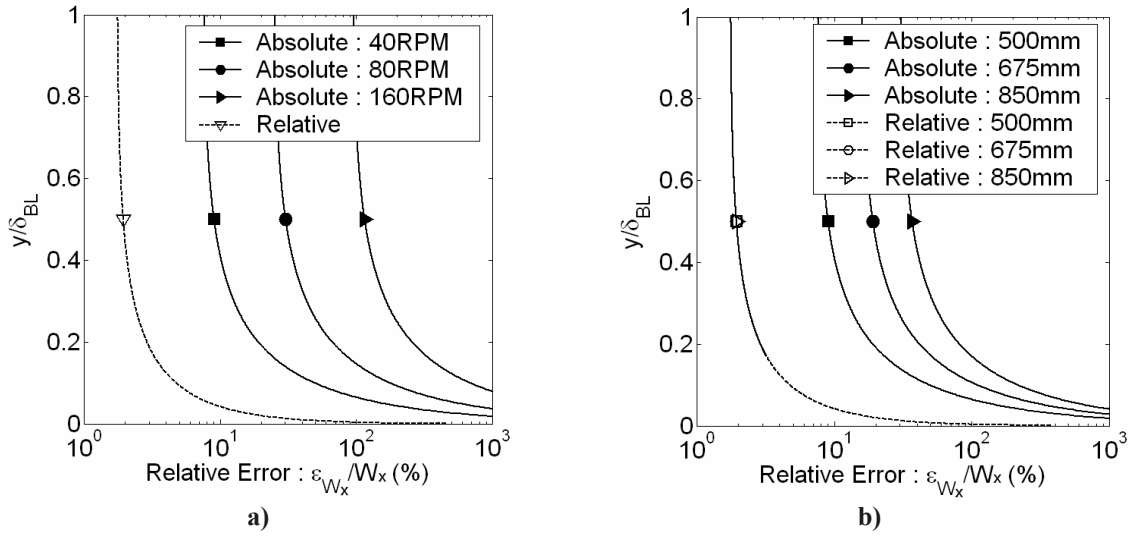

Fig. 6 Relative error on the W_x-component of the relative velocity within the boundary layer when imposing an exponential velocity profile. Measured within an absolute (solid lines) and relative (dashed lines) reference frame a) at different rotational speeds and constant radius b) at 40RPM for different radial coordinates

RESULTS

Instantaneous Flow Field

Following 2-D PIV measurements represent random samples of the SS-PS instantaneous flow field. Figure 7 shows the velocity vector fields and vorticity contour plots in a mid channel height plane at at Ro=0.26 close to the suction (a) and pressure side (d). The rotation results in individual vortices at some distance away from the suction side. The subtraction of the vortex core velocity gives a view of the vector field which is equivalent to the view of an observer moving at the convection velocity. This simple approach of decomposing the field into a constant streamwise convection velocity W_c plus a deviation is based on the fact that Navier-Stokes equations are Galilean invariant. This means that there is no reason to prefer one frame to another and therefore the frame that best visualizes the vector field can be selected [25]. A detailed view on the vortex is shown Fig. 7b.

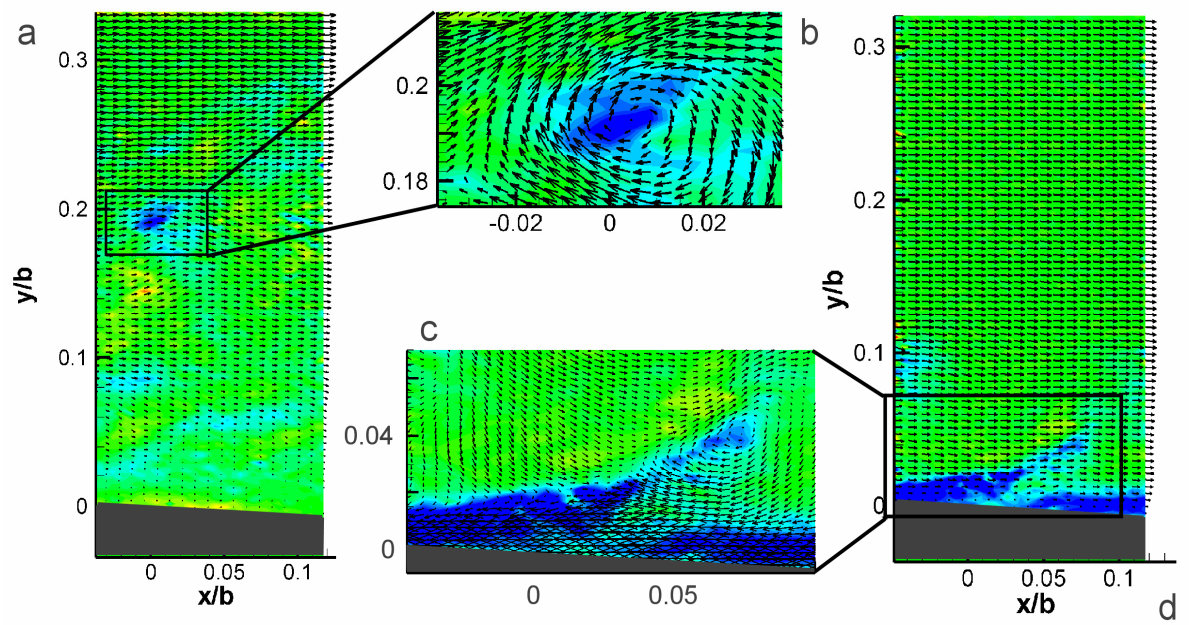

Fig. 7 Instantaneous velocity vector field and vorticity contour plot near suction (a) and pressure side (d) for Ro= 0.26 and detail of the vortical structures after subtraction of the vortex core velocity (b) and (c); in a plane at mid channel height

The vorticity distribution and the velocity vector field on the pressure side show a much more complex pattern (Fig. 7d). Figure 7c and Fig. 8 shows a detail of the instantaneous velocity vector field and the vorticity contour plot after subtraction of the vortex core velocity. They clearly identify the 2-D signature of an hairpin vortex [25,26].

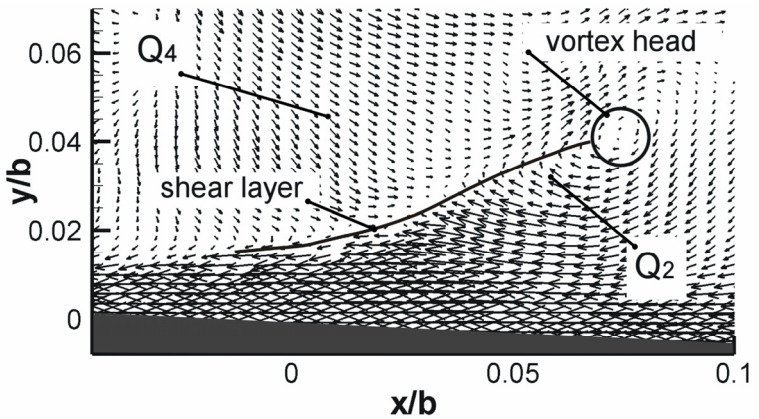

Fig. 8 Hairpin vortex characteristics as measured close to the pressure side at Ro= 0.26 for the plane at mid channel height

Time Resolved Measurements

The time resolved character of the measurements allows tracing the time evolution of the flow and vortices. A wavelet analysis applied to 1000 consecutive flow fields provides the center and radial extension of the vortices for each instantaneous vector field. Superposition of the vortex locations indicates the vortex path (Fig. 9). Vortices are located at two positions near the suction side. A small amount of vortices travels streamwise near the wall. Most of the vortices are located at *'y/l= 0.2'*

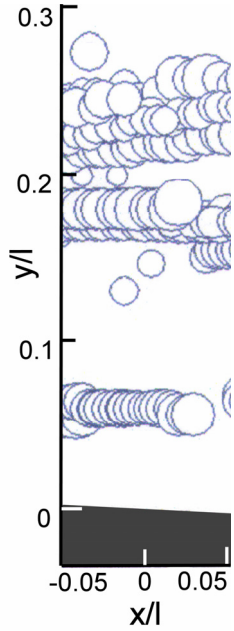

Fig. 9 Vortex transport on the suction side at Ro=0.33

Mean Velocity and Turbulence Intensity Profiles

Mean velocity and turbulence intensity profiles have been obtained by applying the 'dependent circular block bootstrapping' technique. [23]. They are extracted along a line between SS and PS halfway between channel inlet and outlet. Each profile is composed of 460 points along the channel width *'b= 120'* mm.

It appears from Fig. 10 that the boundary layer thickness on the SS increases with rotational speed, while it slightly decreases on the PS. The theoretical potential velocity profile is also plotted in fig. 10b. It shows a larger gradient than the measured one, suggesting a non negligible impact of secondary flows and blockage. The relative measurement error at Ro=.26 remains below 0.5% in the inviscid part of the velocity profiles and increases to a maximum of 15% for the last 5 points close to the suction side (Fig 10). This corresponds to 1% of the whole passage width and these values are not depicted in Fig. 10b for the sake of image readability. The increased error in these points is due to the inaccuracy of the FFT-based correlation algorithm near the walls and a local decrease of the seeding. The relative error remains below 3% near the pressure side,

The mean stream turbulence intensity profile shown on Fig. 11 indicates that at increasing rotation the turbulence intensity peak moves away from the SS while it concentrates closer to the PS. Associated errors remain below 6% in both cases.

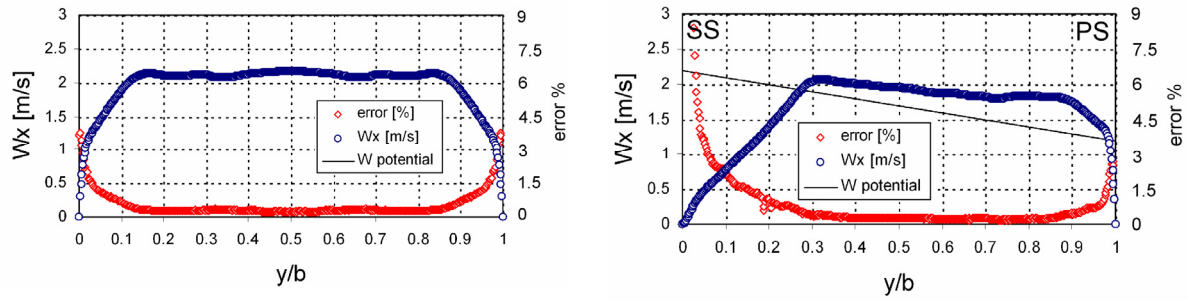

a) **b)**

Fig. 10 Mean stream-wise velocity profiles and associated errors at 95% confidence level, for a) stationary conditions and b) Ro= 0.26

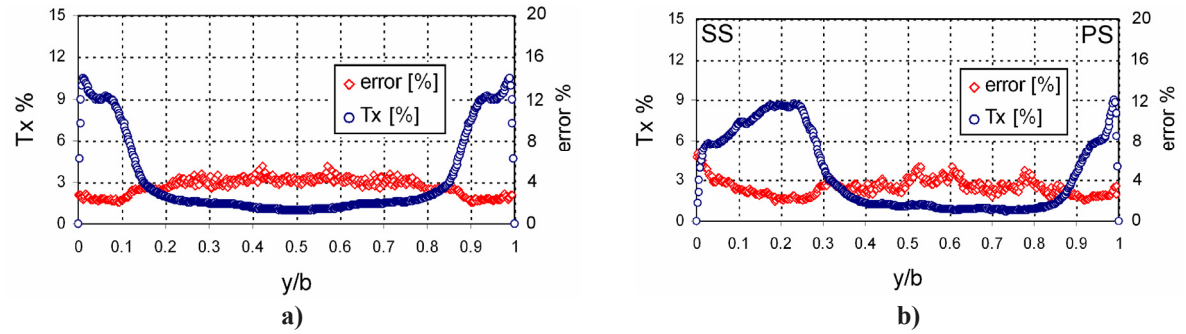

Fig. 11 Mean stream-wise turbulence intensity profiles and associated errors at 95% confidence level, for a) stationary conditions and b) Ro= 0.26

CONCLUSIONS AND FUTURE DEVELOPMENTS

The newly built Rotating Channel facility allows accurate 2-D, Time-Resolved PIV measurements by acquiring the data directly in the rotating frame. This is achieved by mounting the instrumentation together with the channel on a rotating disk. A compact air-cooled laser diode was selected to illuminate the seeding particles. The high-speed camera allows a direct measurement of the velocity thanks to the possibility to store the recorded images in the internal memory. It was demonstrated that the direct acquisition of the relative velocity by this innovative approach allows a large improvement of the accuracy and time accurate PIV flow field measurement.

The impact of rotation on the 2-D boundary layer turbulence structures have for the first time been reported with high spatial and temporal resolution. Hairpin vortices characterize the boundary layer in rotation on the pressure side. The thick boundary layer on the suction side shows circular coherent structures traveling relatively distant from the wall. Turbulence and velocity profiles show a large impact of rotation.

Results shown in this paper are for a divergent channel and are representative for the flow in a radial impeller. Using a parallel walled channel could simulate the flow in the cooling channel of a large HP turbine. Adding roughness and turbulators to the walls is only a minor extension.

All the four walls of the model should be heated to correctly model the real non-adiabatic flow in a micro GT and in internal cooling channels. Indium Tin Oxide ('ITO') is a conductive transparent coating that can be sputtered on thin polyester films or glass. It can be extremely thin (500 angstrom) and permits up to 90% light transmission so that it does not harm the optical access to the flow. It has a high resistance and temperatures of the layer up to 85° C can be obtained by Joule effect. At this temperature it is drawing about 7 kW/m^2. Melting of the polyester walls prohibits higher temperatures.

AKNOWLEDGEMENTS

This research is sponsored by the IWT, the Institute for the Promotion of Innovation by Science and Technology in Flanders; project SBO 030288 "PowerMEMS".

REFERENCES

[1] Johnston JP, (1970) The Effects of Rotation on Boundary Layers in Turbomachine Rotors, Report MD-24, Stanford University, USA.

[2] Johnston JP, (1998) Effects of System Rotation on Turbulence Structure: a Review Relevant to Turbomachinery Flows, International Journal of Rotating Machinery, Vol. 4.

[3] Smirnov P.E., Menter F.R., (2008) Sensitization of the SST Turbulence Model to Rotation and Curvature by Applying the Spalart-Shur Correction Term, ASME GT2008-50480.

[4] Moore J, (1973) A Wake and an Eddy in a Rotating Radial Flow Passage, Part 1: Experimental Observations, ASME Journal of Engineering for Power, Vol. 95, No.3.

[5] Koyama HS, Uchikawa K, Nigim HH, (1997) Effects of Coriolis Force on Flow in Rotating Diffusers, AIAA Journal, Vol. 35, No.7.

[6] Koyama H, Masuda S, Ariga I, Watanabe I, (1979) Stabilizing and Destabilizing Effects of Coriolis Force on Two- Dimensional Laminar and Turbulent Boundary Layers, ASME Journal of Engineering for Power, Vol. 109.

[7] Bons JP, (1998) Complementary Velocity and Heat Transfer Measurements in a Rotating Turbine Cooling Passage, PhD Thesis, MIT, Cambridge, USA.

[8] Bons JP, Kerrebrock JL, (1999) Complementary Velocity and Heat Transfer Measurements in a Rotating Turbine Cooling Passage with Smooth Walls, ASME Journal of Turbomachinery, Vol. 121.
[9] Rau G, Çakan, M, Moeller D, Arts T, (1998) The effect of periodic ribs on the local aerodynamic and heat transfer performance of a straight cooling channel. J. of Turbomachinery (ASME), Vol. 120, No 2, pp 368-375.
[10] Casarsa L, Arts T, (2005) Experimental investigation of the aero-thermal performance of a high blockage rib-roughened cooling channel J. of Turbomachinery (ASME), Vol. 127, pp 580-588.
[11] Paone N, Riethmuller M, Van den Braembussche RA, (1989)Experimental Investigation of the Flow in the Vaneless Diffuser of a Centrifugal Pump by Particle Image Displacement Velocimetry, Exp Fluids, No 7.
[12] Loeherke RI, Nagib HM, (1976) Control of Free Stream Turbulence by Means of Honeycombs: a Balance between Suppression and Generation, ASME Journal of Fluids Engineering, Vol. 98.
[13] Farell C, Youseff S, (1996) Experiments on Turbulence Management Using Screens and Honeycombs, ASME Journal of Fluids Engineering, Vol. 118.
[14] Bharadwaj R, Poncer J, Jacob JD, (2002) PIV Measurements in Ribbed Ducts with and without Rotation, AIAA paper 2002-2738.
[15] Iacovides H, Kounadis D, Launder BE, Li J, Xu Z, (2004) Experimental Study of the Flow and Thermal Development of a Row of Cooling Jets Impinging on a Rotating Concave Surface, ASME GT 2004-53244.
[16] Boxx IG, Idicheria CA, Clemens NT, (2004) Kilohertz PIV/PLMS of Low-gravity Turbulent Flames in a Drop Tower, 12th International Symposium on Applications of Laser Techniques to Fluid Mechanics, Lisbon, Portugal.
[17] Tani N, Kondo H, Mori M, Hishida K, Maeda M, (2002) Development of Fiberscope PIV system by controlling diode laser illumination, Experiments in Fluids No. 33.
[18] www.jold.de
[19] www.visionresearch.com
[20] Keane RD, Adrian RJ, (1990) Optimization of Particle Image Velocimeters. Part I: Double Exposed Systems, Meas. Sci. Technol., 1.
[21] Di Sante A, (2008) Time Resolved PIV Measurements of Low Reynolds number Flow in Rotating Channels, PhD Thesis, von Karman Institute for Fluid Dynamics- Università Politecnica delle Marche, ISBN 978-2-930389-29-X.
[22] Di Sante A, Theunissen R, Van den Braembussche RA, (2008) A New Facility for Time Resolved PIV Measurements in Rotating Channels, Exp Fluids, Vol.44, No. 2, pp.179-188
[23] Theunissen R, Di Sante A, Riethmuller M, Van den Braembussche RA, (2008) Confidence Estimation in the Statistical Analysis of Time-Resolved PIV by Dependent Circular Block Bootstrapping, Experiments in Fluids, Exp Fluids, Vol.44, No. 4, pp.591-596.
[24] Abernethy RB, Benedict RP, Dowdell RB, (1985) Measurement Uncertainty, Journal of Fluids Engineering, Vol. 107.
[25] Adrian RJ, Meinhart CD, Tomkins CD, (2000) Vortex organization in the outer region of the turbulent boundary layer. J Fluid Mech., Vol. 422, pp. 1-54.
[26] Pope S, (2000) Turbulent flows. Cambridge Univ. Press. ISBN 0 521 59886 9